Collaborative Research Center TRR 257
Particle Physics Phenomenology after the Higgs Discovery

Research Training Group
Physics of the Heaviest
Particles at the LHC

RWTH AACHEN UNIVERSITY

Institut für
Theoretische
Teilchenphysik und
Kosmologie

RWTH AACHEN UNIVERSITY

Quark-Mass Effects in Higgs Production

Tom Schellenberger

with M. Czakon, F. Eschment, M. Niggetiedt, R. Ponecelet

Based on Phys.Rev.Lett. 132 (2024) 21, 211902 & JHEP 10 (2024) 210

HIGGS 2024 - Uppsala

Motivation

- Higgs production cross section is central observable
- Gluon fusion channel is the dominant production channel
- Crucial to reduce Theory uncertainties

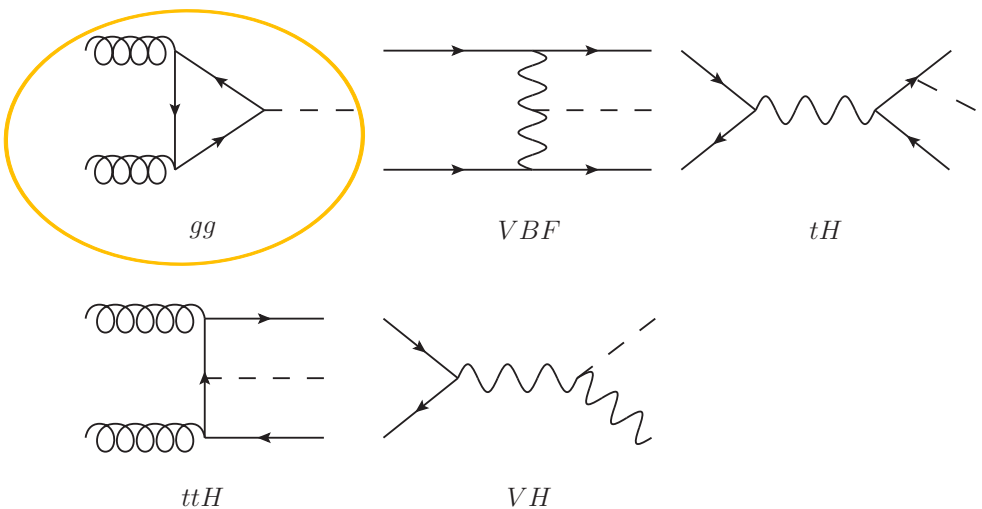

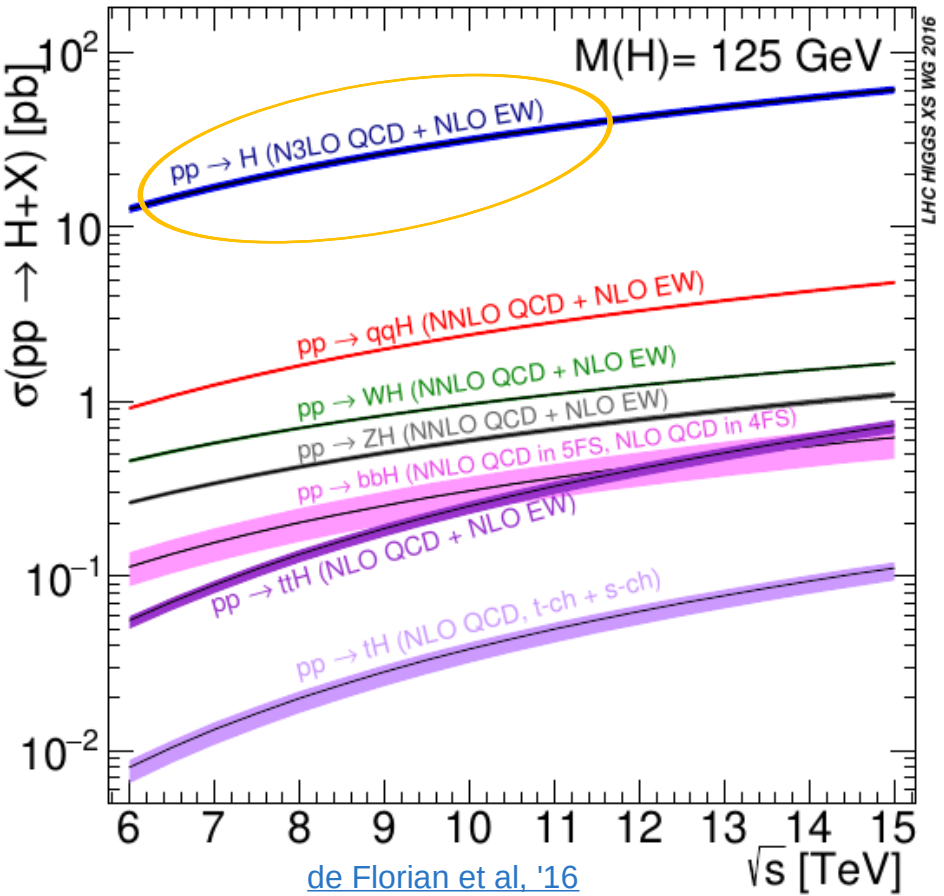

de Florian et al, '16

The Gluon Fusion Channel

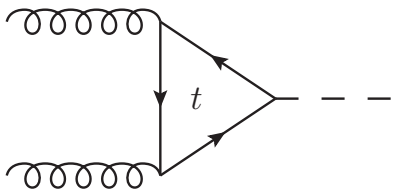

- Gluon-fusion receives large corrections (~100% at NLO)

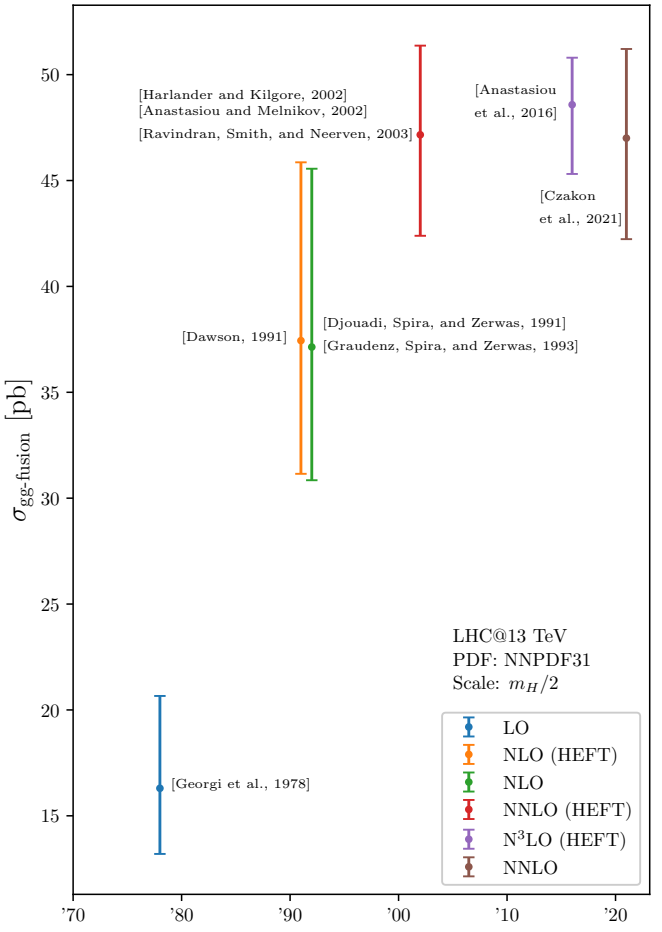

The Gluon Fusion Channel

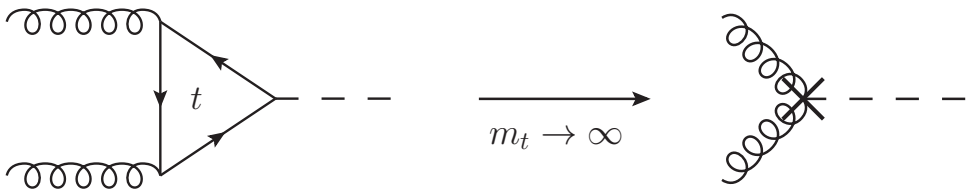

- Gluon-fusion receives large corrections (~100% at NLO)
- Calculations in full QCD are hard! ➡ Instead work in the **Heavy-Top-Limit** (HTL)
  - One less loop
  - One less scale
- Better agreement after rescaling
  - Higgs-Effective-Field-Theory (HEFT)

$$r = \left| \quad \right|^2 \approx 1.065$$

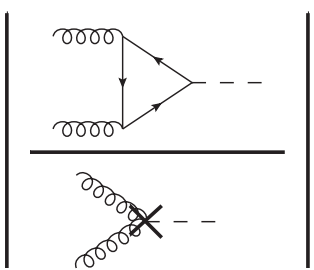

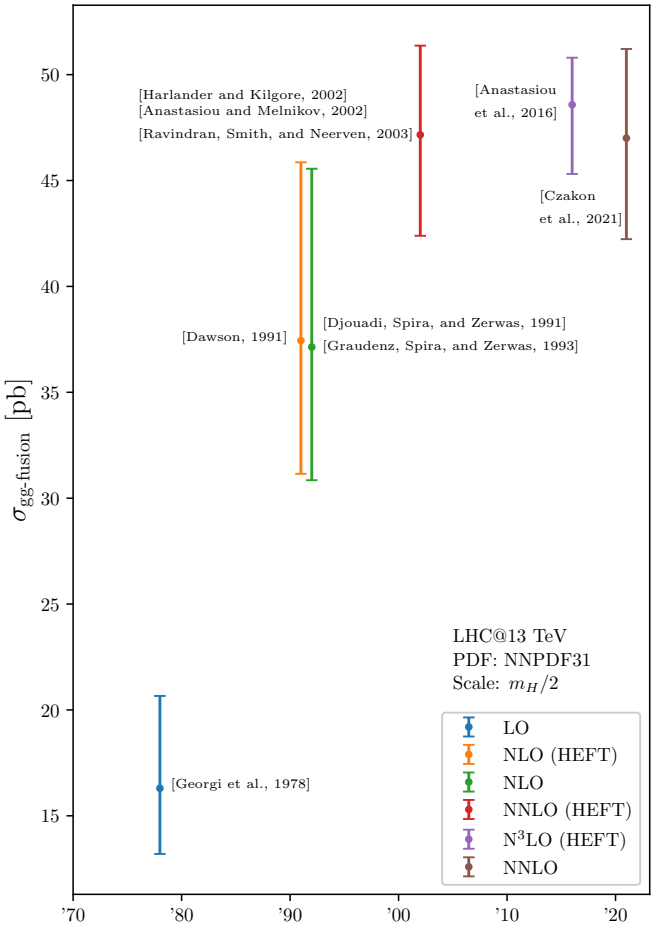

Theory Status

- Current state of the art is **N3LO** Anastasiou et al., 2016

$$\sigma = 48.58\,\text{pb}^{+2.22\,\text{pb}(+4.56\%)}_{-3.27\,\text{pb}(-6.72\%)}\,(\text{theory}) \pm 1.56\,\text{pb}\,(3.20\%)\,(\text{PDF} + \alpha_s)$$

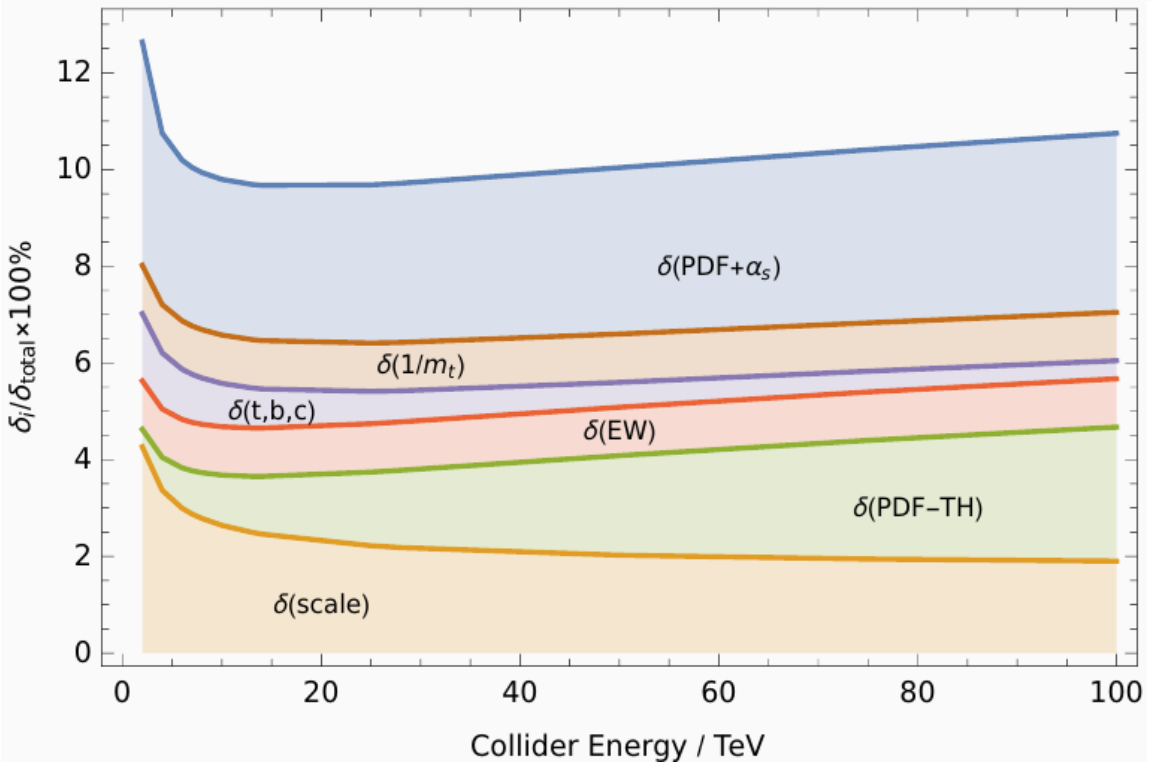

Theory Status

- Current state of the art is **N3LO** Anastasiou et al., 2016

$$\sigma = 48.58\,\text{pb}^{+2.22\,\text{pb}(+4.56\%)}_{-3.27\,\text{pb}(-6.72\%)}\,(\text{theory}) \pm 1.56\,\text{pb}\,(3.20\%)\,(\text{PDF} + \alpha_s)$$

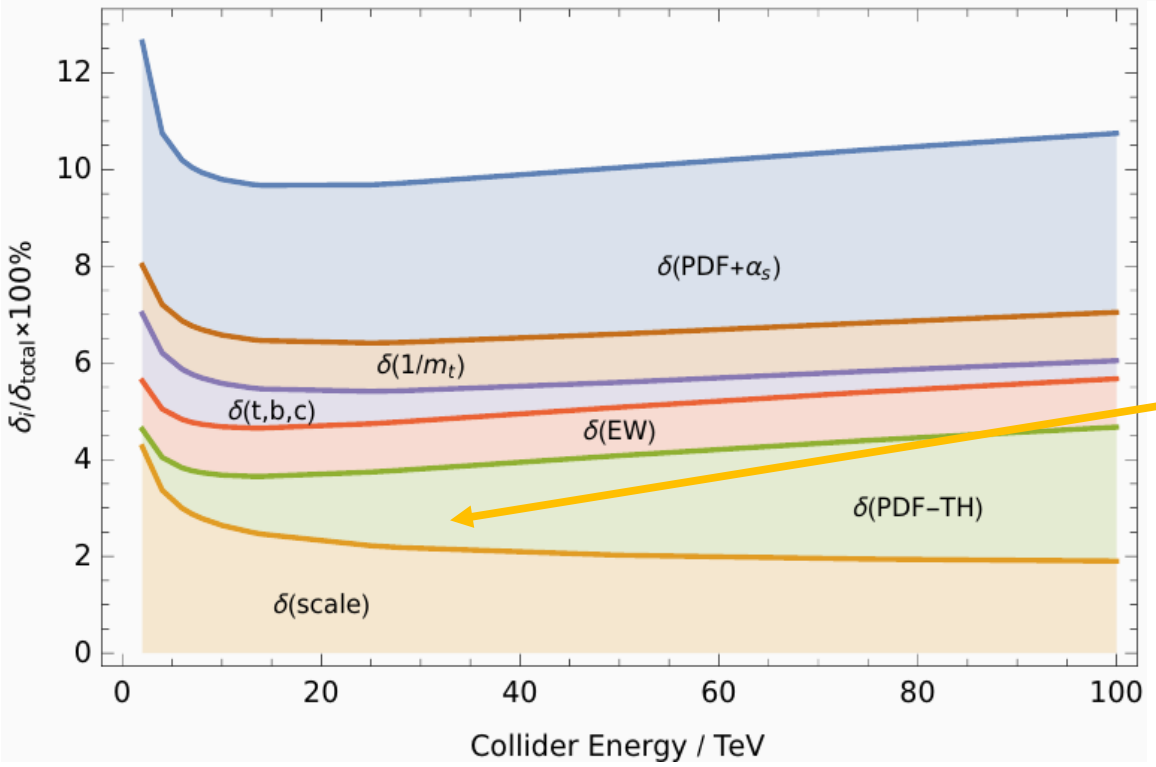

PDFs and their evolution only known at NNLO. Much progress towards N3LO PDF set:

- Moch et al. 2021
- Falcioni et al., 2023
- McGowan et al., 2022
- Ball et al. 2024
- Guan et al., 2024

Theory Status

- Current state of the art is **N3LO** Anastasiou et al., 2016

$$\sigma = 48.58\,\text{pb}^{+2.22\,\text{pb}(+4.56\%)}_{-3.27\,\text{pb}(-6.72\%)}\,(\text{theory}) \pm 1.56\,\text{pb}\,(3.20\%)\,(\text{PDF} + \alpha_s)$$

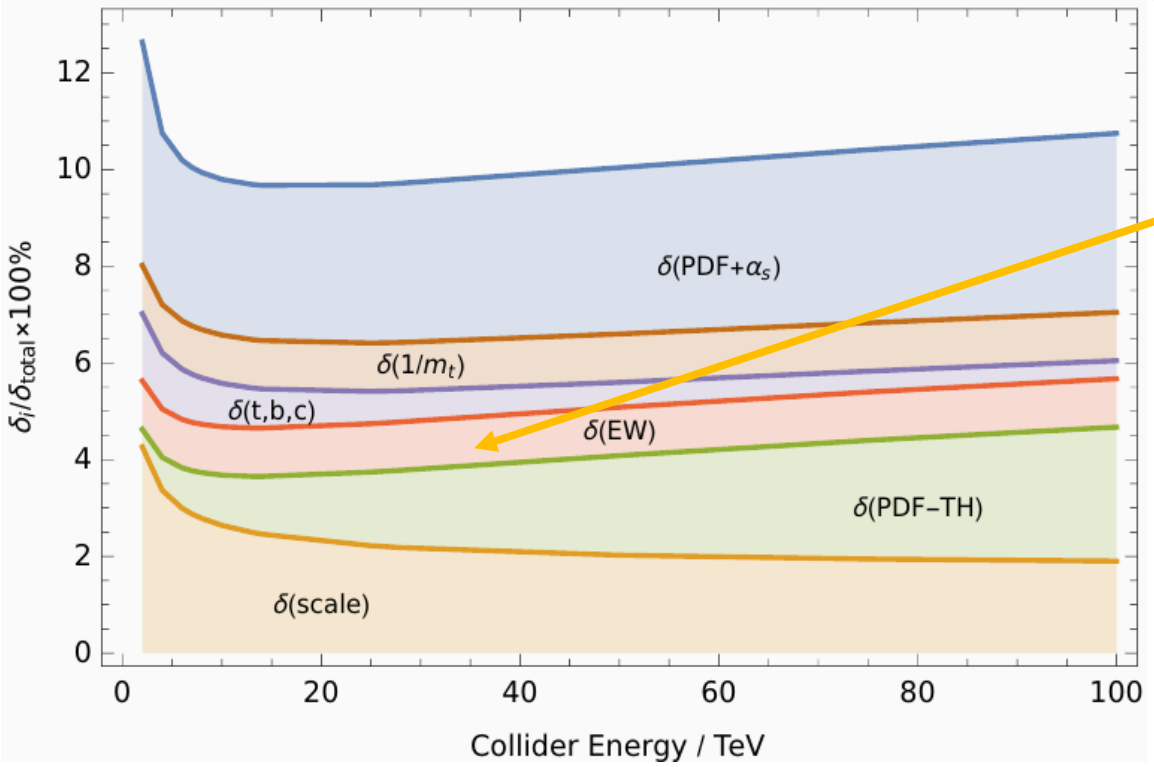

Mixed electro-weak corrections.
Reduced substantially:

- Becchetti et al., 2010
- Becchetti et al., 2021
- Bonetti et al., 2018
- Bonetti et al., 2020
- Bonetti et al., 2022

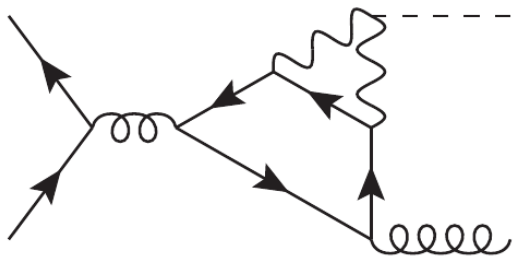

Theory Status

- Current state of the art is **N3LO** Anastasiou et al., 2016

$$\sigma = 48.58\,\text{pb}^{+2.22\,\text{pb}(+4.56\%)}_{-3.27\,\text{pb}(-6.72\%)}\,(\text{theory}) \pm 1.56\,\text{pb}\,(3.20\%)\,(\text{PDF} + \alpha_s)$$

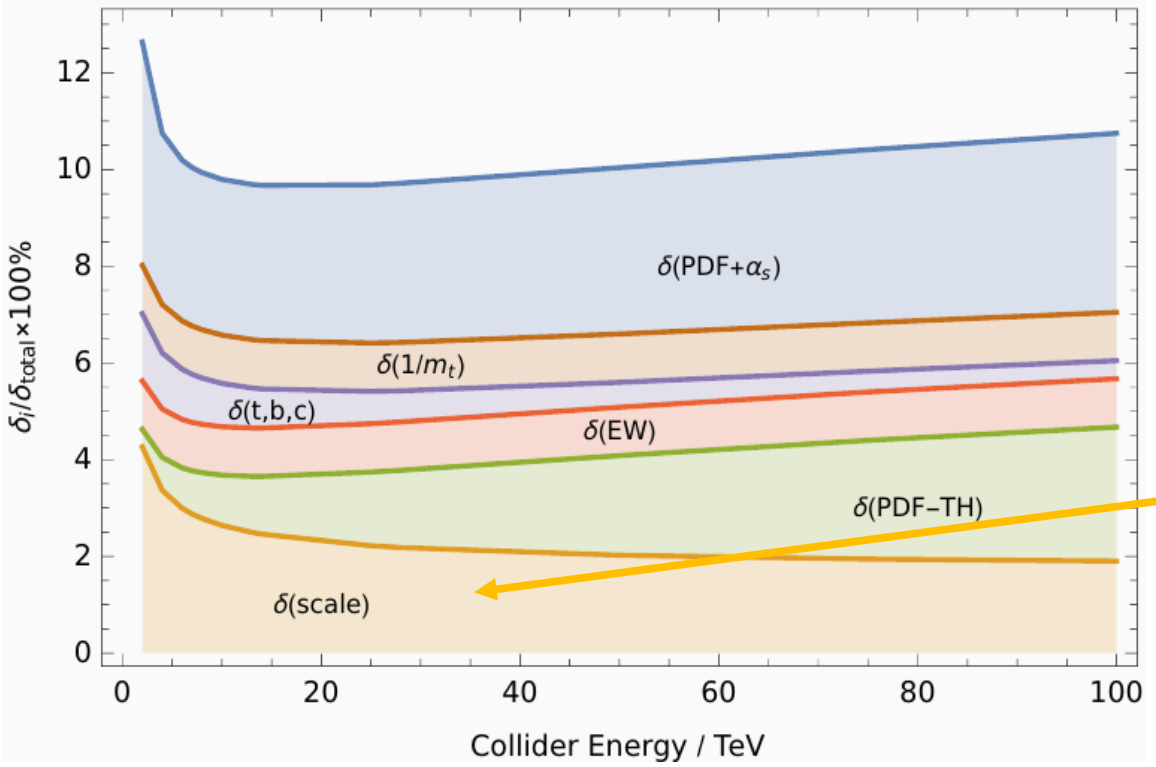

Reduced through N4LO calculation in the soft-virtual approximation:

- Das et al. 2020

Theory Status

- Current state of the art is **N3LO** Anastasiou et al., 2016

$$\sigma = 48.58\,\text{pb}^{+2.22\,\text{pb}(+4.56\%)}_{-3.27\,\text{pb}(-6.72\%)}\,(\text{theory}) \pm 1.56\,\text{pb}\,(3.20\%)\,(\text{PDF} + \alpha_s)$$

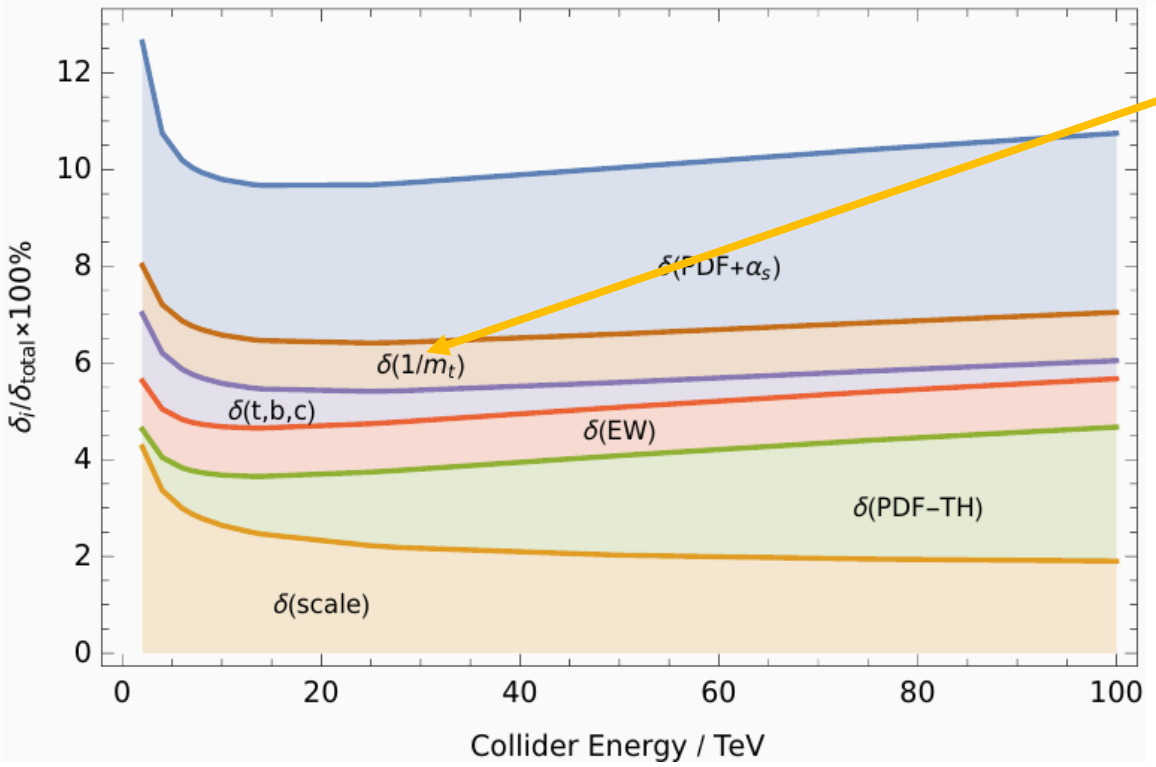

Finite top-mass effects. Basically removed:

- Czakon et al., 2021

Theory Status

- Current state of the art is **N3LO** Anastasiou et al., 2016

$$\sigma = 48.58\,\text{pb}^{+2.22\,\text{pb}(+4.56\%)}_{-3.27\,\text{pb}(-6.72\%)}\,(\text{theory}) \pm 1.56\,\text{pb}\,(3.20\%)\,(\text{PDF} + \alpha_s)$$

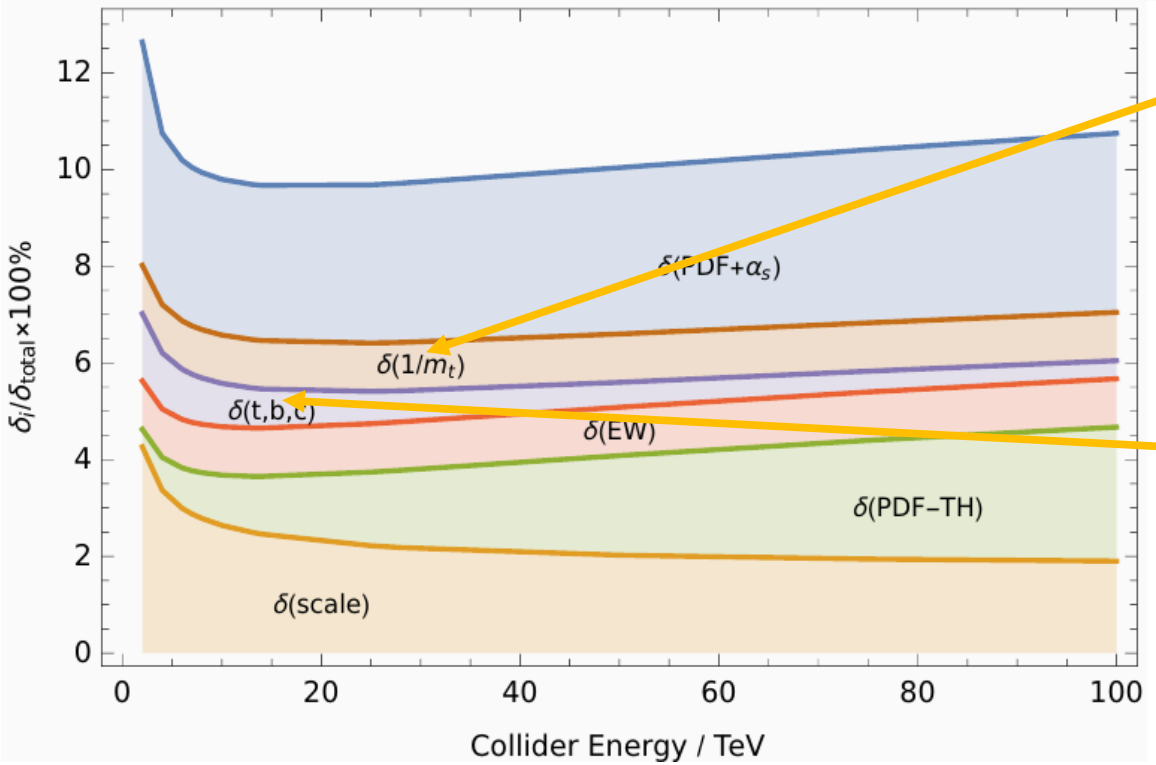

Finite top-mass effects. Basically removed:

- Czakon et al., 2021

Finite bottom and charm quark mass effects. **Our Goal!**

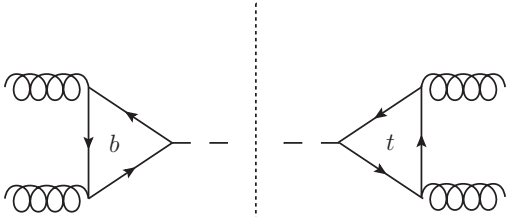

Ingredients for NNLO

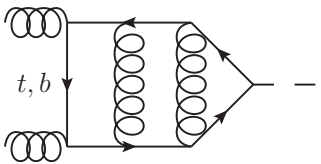

Double-Virtual

- Deep asymptotic expansion in $m_H^2/m_t^2, m_b^2/m_H^2$
- Single massive quark flavor Czakon et al., 2020
- Two massive quark flavors Niggetiedt et al., 2023

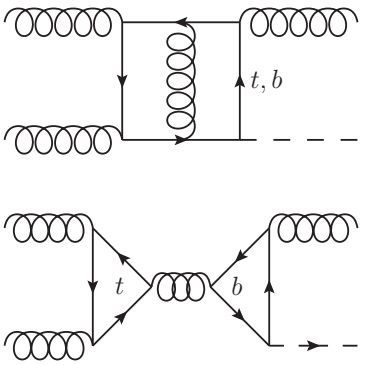

Real-Virtual

- Single massive flavor amplitudes through interpolation of **numerical grid**
- Two different quark flavors result in factorization → One-loop integrals

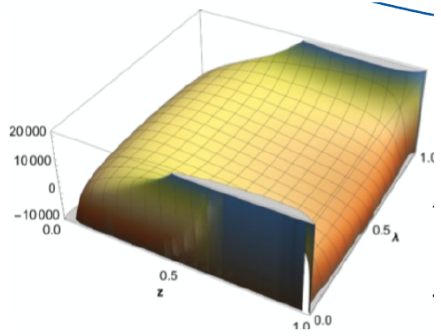

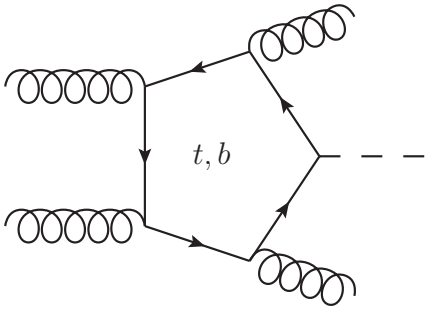

Double-Real

- Calculated in Del Duca et al., 2001
- We use calculation from Budge et al., 2020 as implemented in `MCFM` Campbell et al., 1999
- Scalar integrals with `QCDLOOP` Carrazza et al., 2016

Ingredients for NNLO

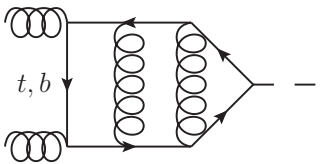

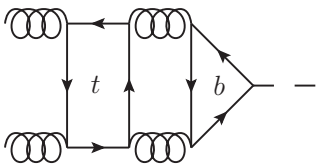

Double-Virtual

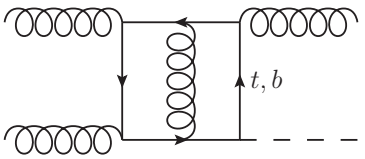

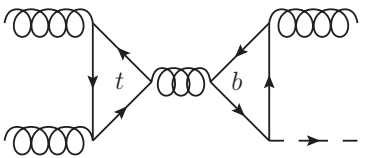

Real-Virtual

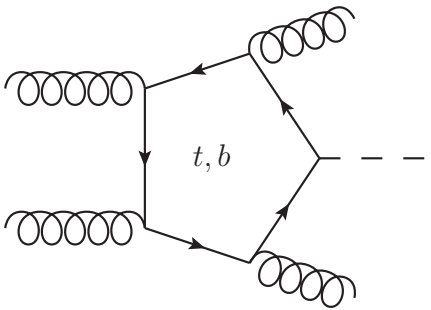

Double-Real

Phase-space integration with sector-imporved residue subtraction (Czakon, 2010) as implemented in C++ code `Stripper`

How to Treat massive b-quarks?

4 Flavor-Scheme (4FS)

- Consistently treat bottom quark as massive
- Exclude bottom-quark from initial state
- Also consider massive bottom-quark radiation

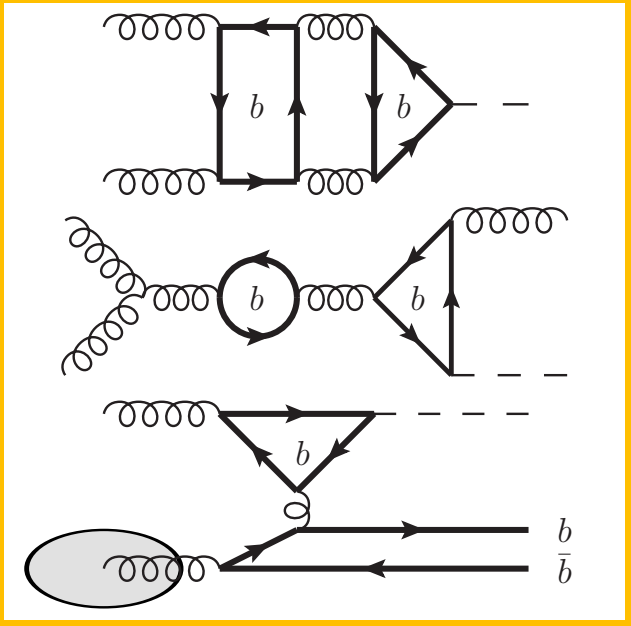

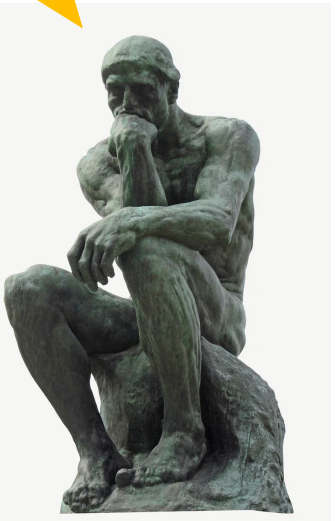

How to Treat massive b-quarks?

4 Flavor-Scheme (4FS)

- Consistently treat bottom quark as massive
- Exclude bottom-quark from initial state
- Also consider massive bottom-quark radiation

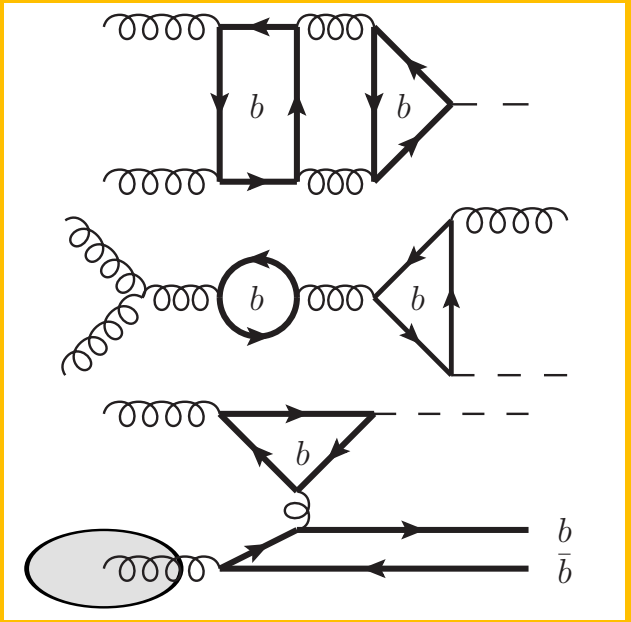

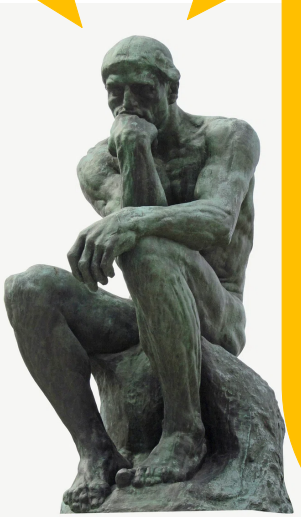

5 Flavor-Scheme (5FS)

- Treat bottom-quark as a massless particle
- Except for **closed** fermion loops that **couple to the Higgs**

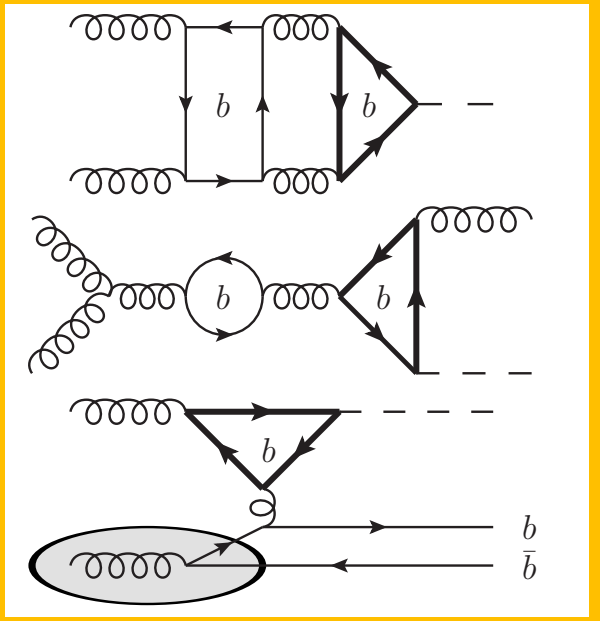

4FS vs 5FS

Order	σ_{HEFT} [pb]				
	$\sqrt{s} = 13$ TeV				
	5FS	4FS $m_b = 0.01$ GeV	4FS $m_b = 0.1$ GeV	4FS $m_b = 4.78$ GeV	4FS $\overline{m}_b(\overline{m}_b) = 4.18$ GeV
$\mathcal{O}(\alpha_s^2)$	$+16.30$	$+16.27$	$+16.27$	$+16.27$	16.27
LO	$16.30^{+4.36}_{-3.10}$	$16.27^{+4.63}_{-3.22}$	$16.27^{+4.63}_{-3.22}$	$16.27^{+4.63}_{-3.22}$	$16.27^{+4.63}_{-3.22}$
$\mathcal{O}(\alpha_s^3)$	$+21.14$	$+20.08(3)$	$+20.08(3)$	$+20.08(3)$	$+20.08(3)$
NLO	$37.44^{+8.42}_{-6.29}$	$36.35(3)^{+8.57}_{-6.32}$	$36.35(3)^{+8.57}_{-6.32}$	$36.35(3)^{+8.57}_{-6.32}$	$36.35(3)^{+8.57}_{-6.32}$
$\mathcal{O}(\alpha_s^4)$	$+9.72$	$+10.8(4)$	$+11.1(4)$	$+9.5(2)$	$+9.6(2)$
NNLO	$47.16^{+4.21}_{-4.77}$	$47.2(4)^{+5.4}_{-5.4}$	$47.5(4)^{+5.4}_{-5.5}$	$45.9(2)^{+4.3}_{-4.9}$	$46.0(2)^{+4.4}_{-5.0}$

4FS vs 5FS

Order	σ_{HEFT} [pb]				
	$\sqrt{s} = 13$ TeV				
	5FS	4FS $m_b = 0.01$ GeV	4FS $m_b = 0.1$ GeV	4FS $m_b = 4.78$ GeV	4FS $\overline{m}_b(\overline{m}_b) = 4.18$ GeV
$\mathcal{O}(\alpha_s^2)$	$+16.30$	$+16.27$	$+16.27$	$+16.27$	16.27
LO	$16.30^{+4.36}_{-3.10}$	$16.27^{+4.63}_{-3.22}$	$16.27^{+4.63}_{-3.22}$	$16.27^{+4.63}_{-3.22}$	$16.27^{+4.63}_{-3.22}$
$\mathcal{O}(\alpha_s^3)$	$+21.14$	$+20.08(3)$	$+20.08(3)$	$+20.08(3)$	$+20.08(3)$
NLO	$37.44^{+8.42}_{-6.29}$	$36.35(3)^{+8.57}_{-6.32}$	$36.35(3)^{+8.57}_{-6.32}$	$36.35(3)^{+8.57}_{-6.32}$	$36.35(3)^{+8.57}_{-6.32}$
$\mathcal{O}(\alpha_s^4)$	$+9.72$	$+10.8(4)$	$+11.1(4)$	$+9.5(2)$	$+9.6(2)$
NNLO	$47.16^{+4.21}_{-4.77}$	$47.2(4)^{+5.4}_{-5.4}$	$47.5(4)^{+5.4}_{-5.5}$	$45.9(2)^{+4.3}_{-4.9}$	$46.0(2)^{+4.4}_{-5.0}$

- Difference at LO only caused by normalization of the PDFs

4FS vs 5FS

Order	σ_{HEFT} [pb]				
	$\sqrt{s} = 13$ TeV				
	5FS	4FS $m_b = 0.01$ GeV	4FS $m_b = 0.1$ GeV	4FS $m_b = 4.78$ GeV	4FS $\overline{m}_b(\overline{m}_b) = 4.18$ GeV
$\mathcal{O}(\alpha_s^2)$	$+16.30$	$+16.27$	$+16.27$	$+16.27$	16.27
LO	$16.30^{+4.36}_{-3.10}$	$16.27^{+4.63}_{-3.22}$	$16.27^{+4.63}_{-3.22}$	$16.27^{+4.63}_{-3.22}$	$16.27^{+4.63}_{-3.22}$
$\mathcal{O}(\alpha_s^3)$	$+21.14$	$+20.08(3)$	$+20.08(3)$	$+20.08(3)$	$+20.08(3)$
NLO	$37.44^{+8.42}_{-6.29}$	$36.35(3)^{+8.57}_{-6.32}$	$36.35(3)^{+8.57}_{-6.32}$	$36.35(3)^{+8.57}_{-6.32}$	$36.35(3)^{+8.57}_{-6.32}$
$\mathcal{O}(\alpha_s^4)$	$+9.72$	$+10.8(4)$	$+11.1(4)$	$+9.5(2)$	$+9.6(2)$
NNLO	$47.16^{+4.21}_{-4.77}$	$47.2(4)^{+5.4}_{-5.4}$	$47.5(4)^{+5.4}_{-5.5}$	$45.9(2)^{+4.3}_{-4.9}$	$46.0(2)^{+4.4}_{-5.0}$

- Difference at LO only caused by normalization of the PDFs
- More significant difference at NLO because additional channel opens up

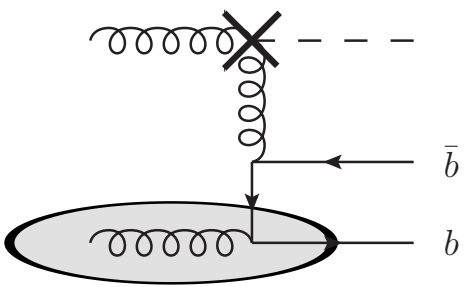

4FS vs 5FS

Order	σ_{HEFT} [pb]				
	$\sqrt{s} = 13$ TeV				
	5FS	4FS $m_b = 0.01$ GeV	4FS $m_b = 0.1$ GeV	4FS $m_b = 4.78$ GeV	4FS $\overline{m}_b(\overline{m}_b) = 4.18$ GeV
$\mathcal{O}(\alpha_s^2)$	$+16.30$	$+16.27$	$+16.27$	$+16.27$	16.27
LO	$16.30^{+4.36}_{-3.10}$	$16.27^{+4.63}_{-3.22}$	$16.27^{+4.63}_{-3.22}$	$16.27^{+4.63}_{-3.22}$	$16.27^{+4.63}_{-3.22}$
$\mathcal{O}(\alpha_s^3)$	$+21.14$	$+20.08(3)$	$+20.08(3)$	$+20.08(3)$	$+20.08(3)$
NLO	$37.44^{+8.42}_{-6.29}$	$36.35(3)^{+8.57}_{-6.32}$	$36.35(3)^{+8.57}_{-6.32}$	$36.35(3)^{+8.57}_{-6.32}$	$36.35(3)^{+8.57}_{-6.32}$
$\mathcal{O}(\alpha_s^4)$	$+9.72$	$+10.8(4)$	$+11.1(4)$	$+9.5(2)$	$+9.6(2)$
NNLO	$47.16^{+4.21}_{-4.77}$	$47.2(4)^{+5.4}_{-5.4}$	$47.5(4)^{+5.4}_{-5.5}$	$45.9(2)^{+4.3}_{-4.9}$	$46.0(2)^{+4.4}_{-5.0}$

- Difference at LO only caused by normalization of the PDFs
- More significant difference at NLO because additional channel opens up
- At NNLO we have real mass dependence
  - Nice convergence for $m_b \to 0$
  - Effect of finite m_b is ~3%, order of magnitude as estimated in Pietrulewicz et al., 2023

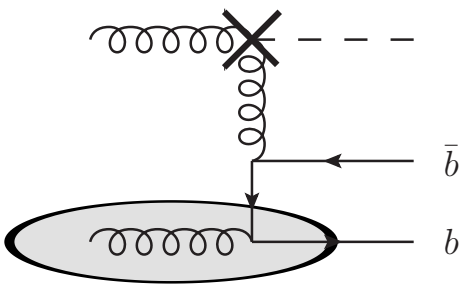

Mass renormalization?

On-shell Scheme

- Renormalized mass is the pole mass
- Mass is constant

$\overline{\text{MS}}$ Scheme

- Only remove divergent parts
- Mass is now running

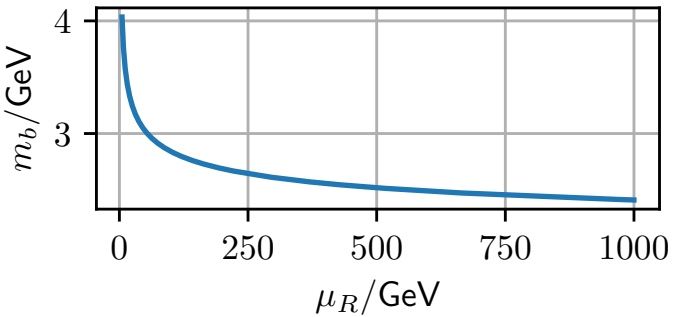

Mass renormalization?

On-shell Scheme

- Renormalized mass is the pole mass
- Mass is constant

$$Z_m^{\overline{\text{MS}}}\overline{m} = Z_m^{\text{OS}} m^{\text{OS}}$$

$$m^{\text{OS}} = \overline{m}\left(1 + c_1\frac{\alpha_s}{\pi} + c_2\left(\frac{\alpha_s}{\pi}\right)^2 + \mathcal{O}(\alpha^3)\right)$$

Gray et al., 1990

Consistency with flavor scheme!

$\overline{\text{MS}}$ Scheme

- Only remove divergent parts
- Mass is now running

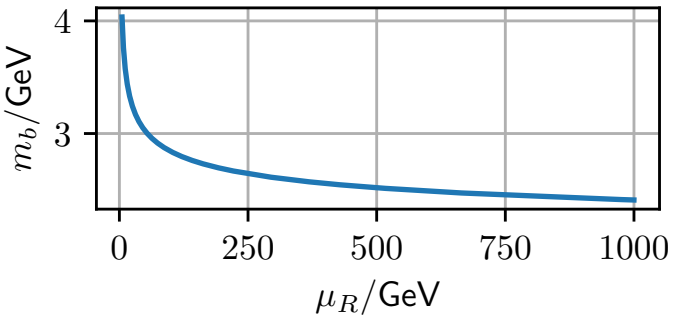

Mass renormalization?

On-shell Scheme

- Renormalized mass is the pole mass
- Mass is constant

$$Z_m^{\overline{\text{MS}}}\overline{m} = Z_m^{\text{OS}} m^{\text{OS}}$$

$$m^{\text{OS}} = \overline{m}\left(1 + c_1\frac{\alpha_s}{\pi} + c_2\left(\frac{\alpha_s}{\pi}\right)^2 + \mathcal{O}(\alpha^3)\right)$$

Gray et al., 1990

Consistency with flavor scheme!

$\overline{\text{MS}}$ Scheme

- Only remove divergent parts
- Mass is now running

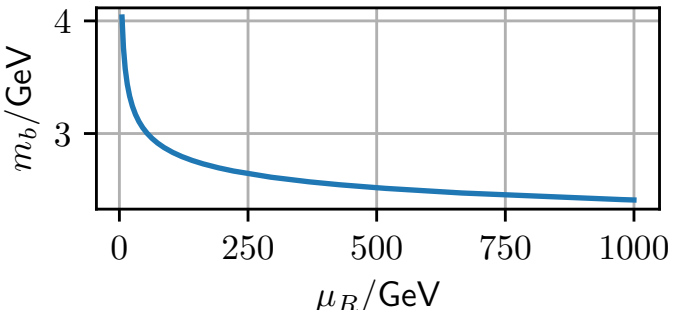

$$\mathcal{M}^{\overline{\text{MS}}} = \mathcal{M}^{\text{OS}} + \delta\mathcal{M},$$

$$\delta\mathcal{M}^{(1)} = \overline{m}c_1\frac{\alpha_s}{\pi}\frac{\mathrm{d}\mathcal{M}^{\text{OS},(0)}}{\mathrm{d}m}\bigg|_{m=\overline{m}},$$

$$\delta\mathcal{M}^{(2)} = \overline{m}\left[c_1\frac{\alpha_s}{\pi}\frac{\mathrm{d}\mathcal{M}^{\text{OS},(1)}}{\mathrm{d}m}\bigg|_{m=\overline{m}} + c_2\left(\frac{\alpha_s}{\pi}\right)^2\frac{\mathrm{d}\mathcal{M}^{\text{OS},(0)}}{\mathrm{d}m}\bigg|_{m=\overline{m}}\right] + \frac{1}{2}\left(\overline{m}c_1\frac{\alpha_s}{\pi}\right)^2\frac{\mathrm{d}^2\mathcal{M}^{\text{OS},(0)}}{\mathrm{d}m^2}\bigg|_{m=\overline{m}}$$

Results

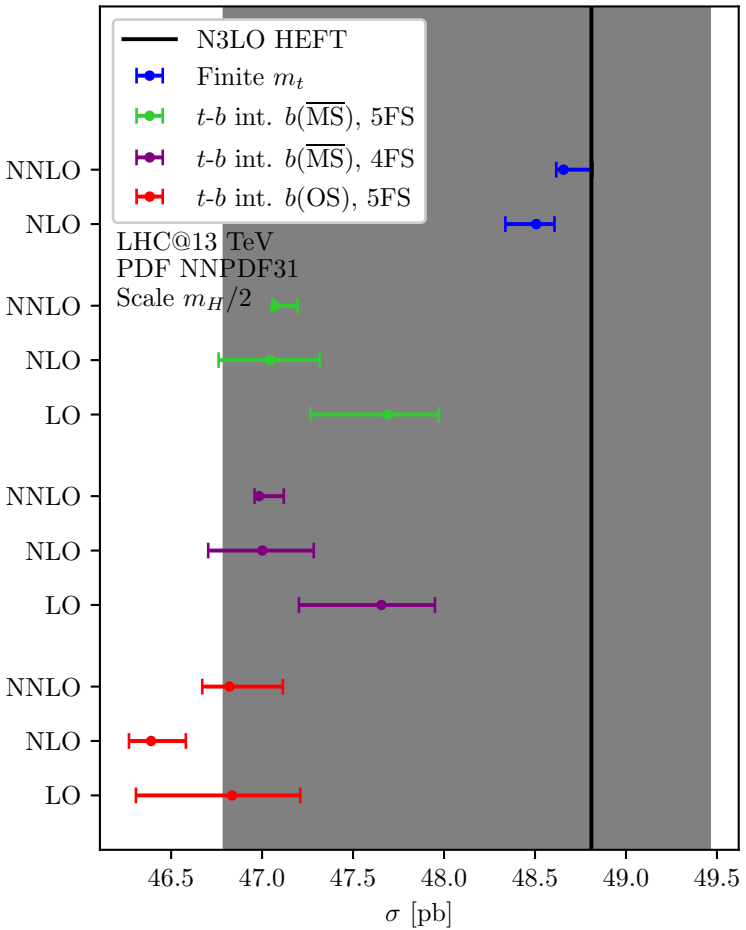

Order	$(\sigma_t^{\overline{\text{MS}}} - \sigma_t^{\text{OS}})$ [pb]
$\sqrt{s} = 13$ TeV	
$\mathcal{O}(\alpha_s^2)$	-0.04
LO	$-0.04^{+0.12}_{-0.17}$
$\mathcal{O}(\alpha_s^3)$	$+0.02$
NLO	$-0.02^{+0.14}_{-0.30}$
$\mathcal{O}(\alpha_s^4)$	$+0.01$
NNLO	$-0.01^{+0.12}_{-0.24}$

$m_H = 125\,\text{GeV}$
$m_t = 173.1\,\text{GeV}$
$m_t(m_t) = 162.7\,\text{GeV}$
$m_b = 4.78\,\text{GeV}$
$m_b(m_b) = 4.18\,\text{GeV}$

Results

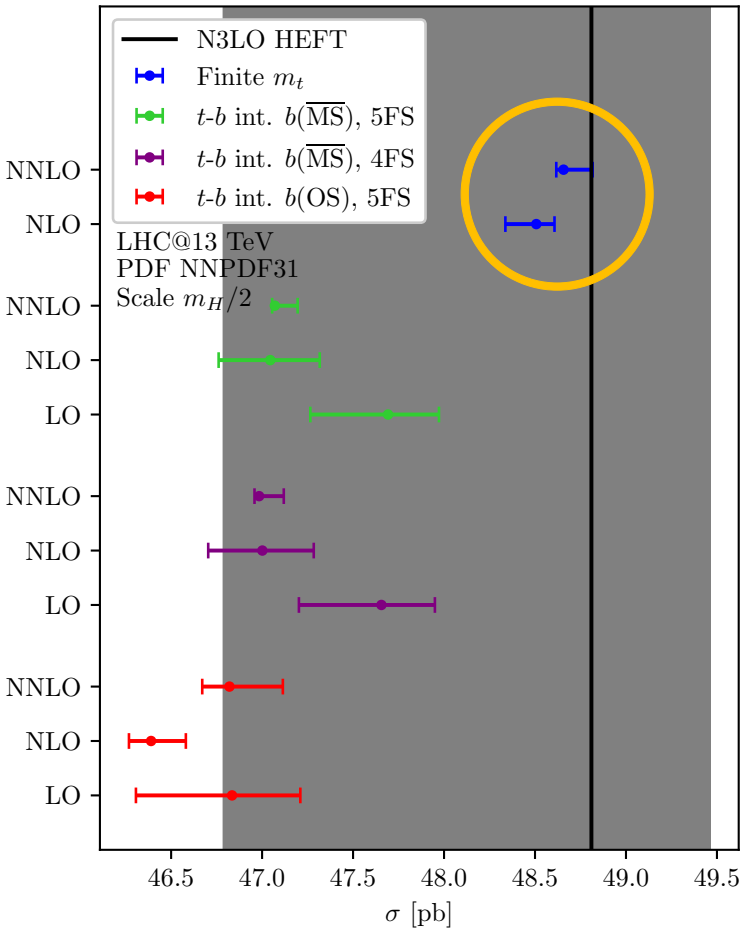

Order	$(\sigma_t^{\overline{\text{MS}}} - \sigma_t^{\text{OS}})$ [pb]
$\sqrt{s} = 13$ TeV	
$\mathcal{O}(\alpha_s^2)$	-0.04
LO	$-0.04^{+0.12}_{-0.17}$
$\mathcal{O}(\alpha_s^3)$	$+0.02$
NLO	$-0.02^{+0.14}_{-0.30}$
$\mathcal{O}(\alpha_s^4)$	$+0.01$
NNLO	$-0.01^{+0.12}_{-0.24}$

$m_H = 125\,\text{GeV}$
$m_t = 173.1\,\text{GeV}$
$m_t(m_t) = 162.7\,\text{GeV}$
$m_b = 4.78\,\text{GeV}$
$m_b(m_b) = 4.18\,\text{GeV}$

- Finite top-mass effects are small
  - The renormalization schemes of the top-quark mass are almost identical!

Results

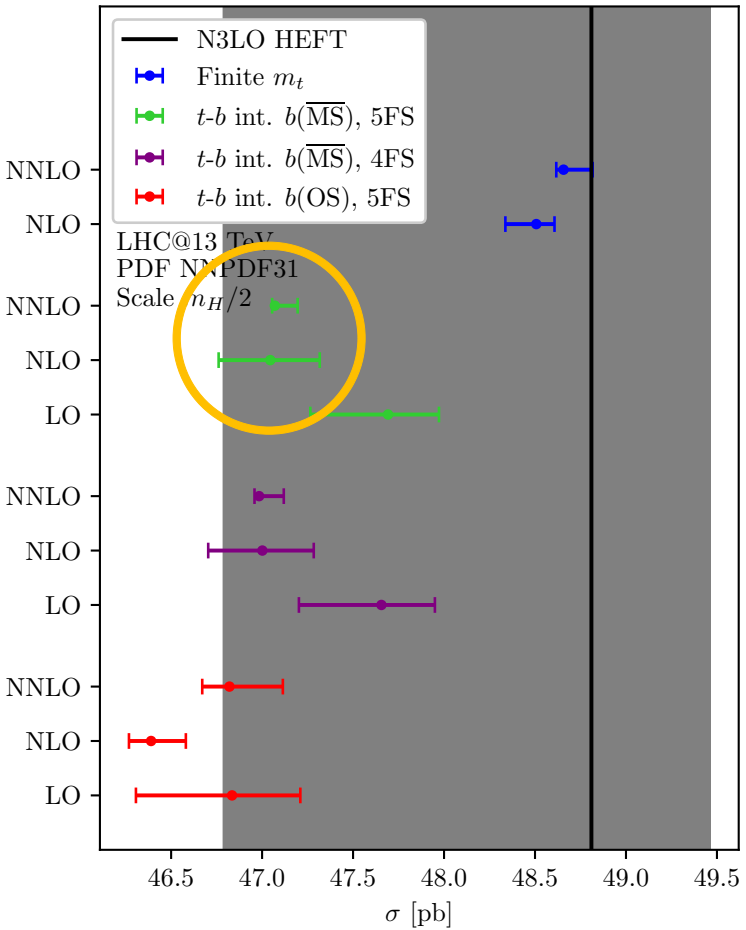

Order	$(\sigma_t^{\overline{\text{MS}}} - \sigma_t^{\text{OS}})$ [pb]
$\sqrt{s} = 13$ TeV	
$\mathcal{O}(\alpha_s^2)$	-0.04
LO	$-0.04^{+0.12}_{-0.17}$
$\mathcal{O}(\alpha_s^3)$	$+0.02$
NLO	$-0.02^{+0.14}_{-0.30}$
$\mathcal{O}(\alpha_s^4)$	$+0.01$
NNLO	$-0.01^{+0.12}_{-0.24}$

$m_H = 125\,\text{GeV}$
$m_t = 173.1\,\text{GeV}$
$m_t(m_t) = 162.7\,\text{GeV}$
$m_b = 4.78\,\text{GeV}$
$m_b(m_b) = 4.18\,\text{GeV}$

- Finite top-mass effects are small
  - The renormalization schemes of the top-quark mass are almost identical!
- Scale uncertainties for top-bottom interference contribution are reduced significantly

Results

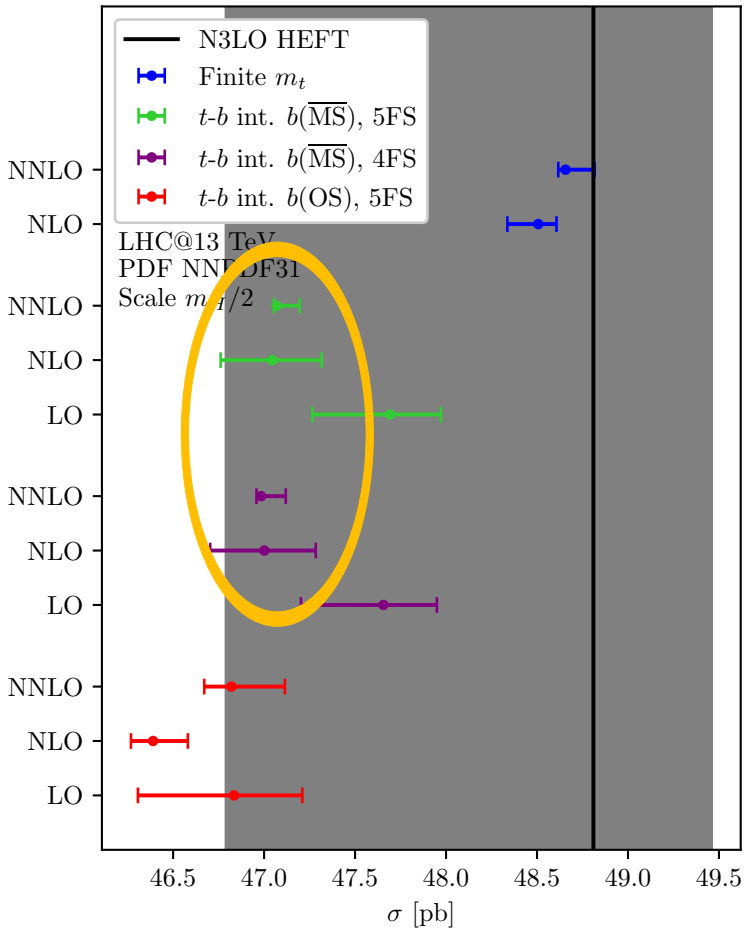

Order	$(\sigma_t^{\overline{\text{MS}}} - \sigma_t^{\text{OS}})$ [pb]
$\sqrt{s} = 13$ TeV	
$\mathcal{O}(\alpha_s^2)$	-0.04
LO	$-0.04^{+0.12}_{-0.17}$
$\mathcal{O}(\alpha_s^3)$	$+0.02$
NLO	$-0.02^{+0.14}_{-0.30}$
$\mathcal{O}(\alpha_s^4)$	$+0.01$
NNLO	$-0.01^{+0.12}_{-0.24}$

$m_H = 125\,\text{GeV}$
$m_t = 173.1\,\text{GeV}$
$m_t(m_t) = 162.7\,\text{GeV}$
$m_b = 4.78\,\text{GeV}$
$m_b(m_b) = 4.18\,\text{GeV}$

- Finite top-mass effects are small
  - The renormalization schemes of the top-quark mass are almost identical!
- Scale uncertainties for top-bottom interference contribution are reduced significantly
- Influence of the flavor scheme on the top-bottom interference is negligible

Results

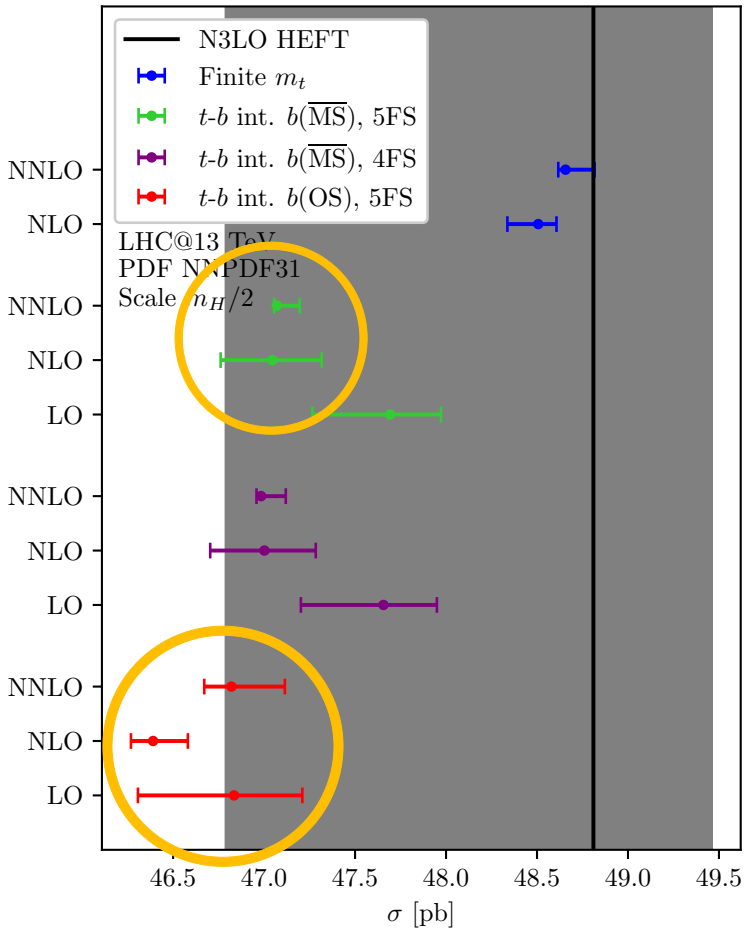

Order	$(\sigma_t^{\overline{\text{MS}}} - \sigma_t^{\text{OS}})$ [pb]
$\sqrt{s} = 13$ TeV	
$\mathcal{O}(\alpha_s^2)$	-0.04
LO	$-0.04^{+0.12}_{-0.17}$
$\mathcal{O}(\alpha_s^3)$	$+0.02$
NLO	$-0.02^{+0.14}_{-0.30}$
$\mathcal{O}(\alpha_s^4)$	$+0.01$
NNLO	$-0.01^{+0.12}_{-0.24}$

$m_H = 125\,\text{GeV}$
$m_t = 173.1\,\text{GeV}$
$m_t(m_t) = 162.7\,\text{GeV}$
$m_b = 4.78\,\text{GeV}$
$m_b(m_b) = 4.18\,\text{GeV}$

- Finite top-mass effects are small
  - The renormalization schemes of the top-quark mass are almost identical!
- Scale uncertainties for top-bottom interference contribution are reduced significantly
- Influence of the flavor scheme on the top-bottom interference is negligible
- MS-scheme shows much better perturbative convergence + smaller scale uncertainties
  - Results are compatible withing scale uncertainties

Top-Bottom Interference Effects

$$H_T = \sqrt{m_H^2 + p_T^2} + \sum_i |p_{i,T}|$$

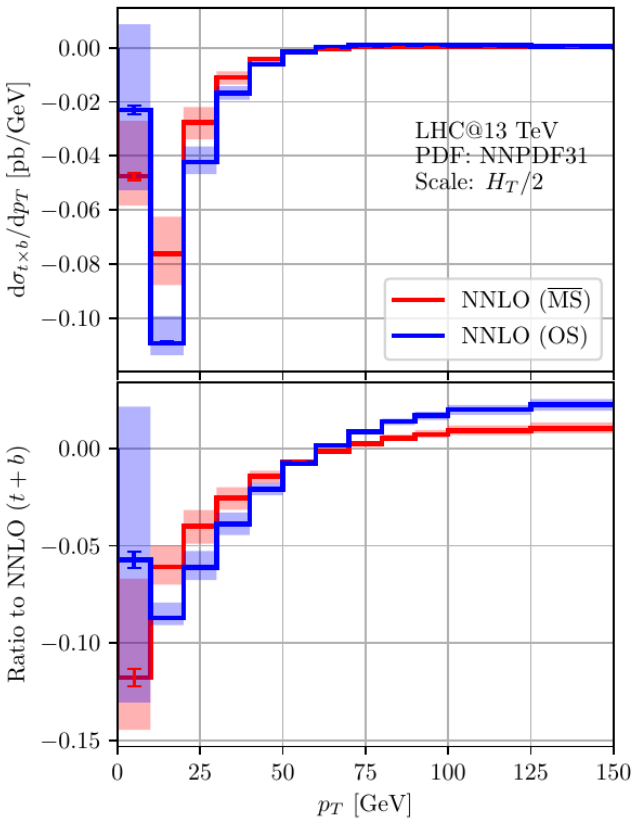

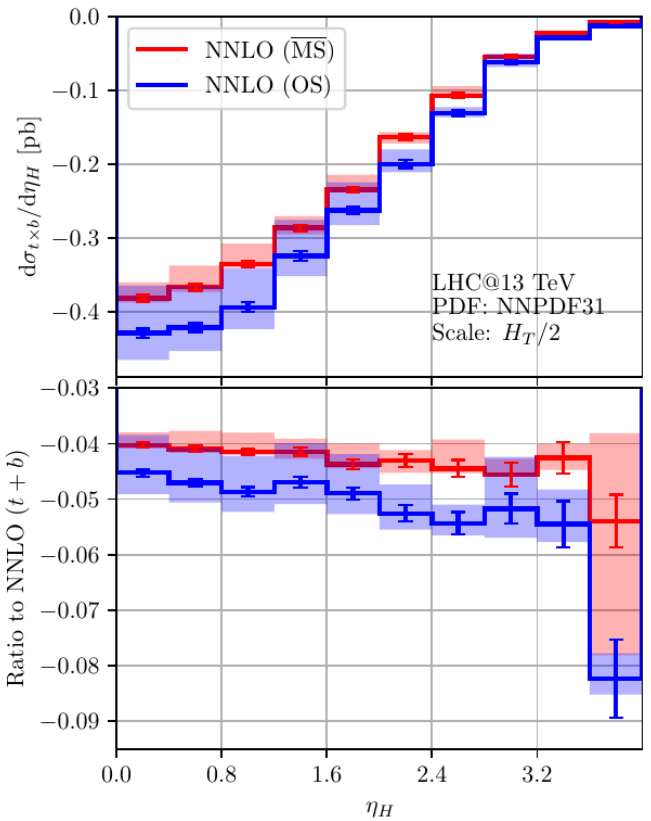

- p_T -distribution known (except for the zero-bin) and we find good agreement
  - Lindert et al., 2017
  - Caola et al., 2018
  - Bonciani et al., 2022
- Rapidity distributions constitute new results

Top-Bottom Interference Effects

$$H_T = \sqrt{m_H^2 + p_T^2} + \sum_i |p_{i,T}|$$

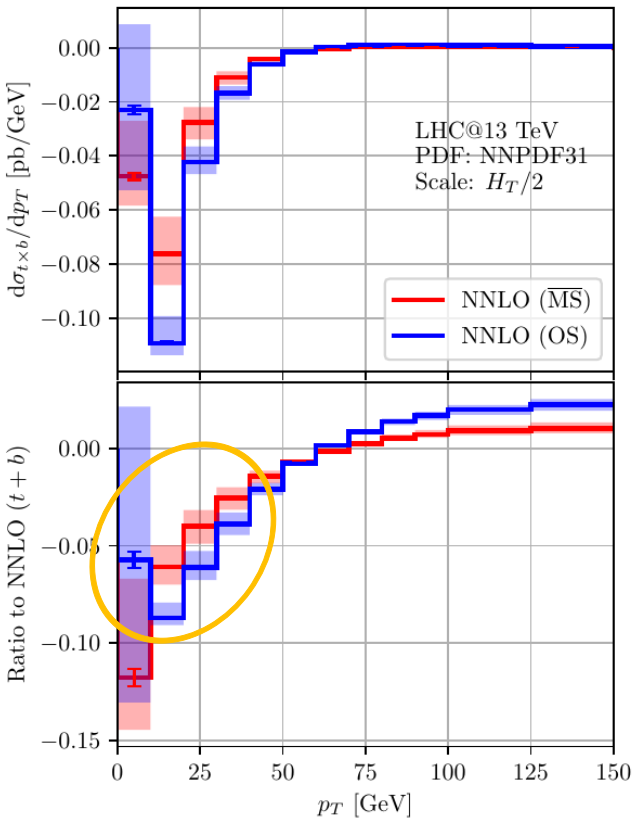

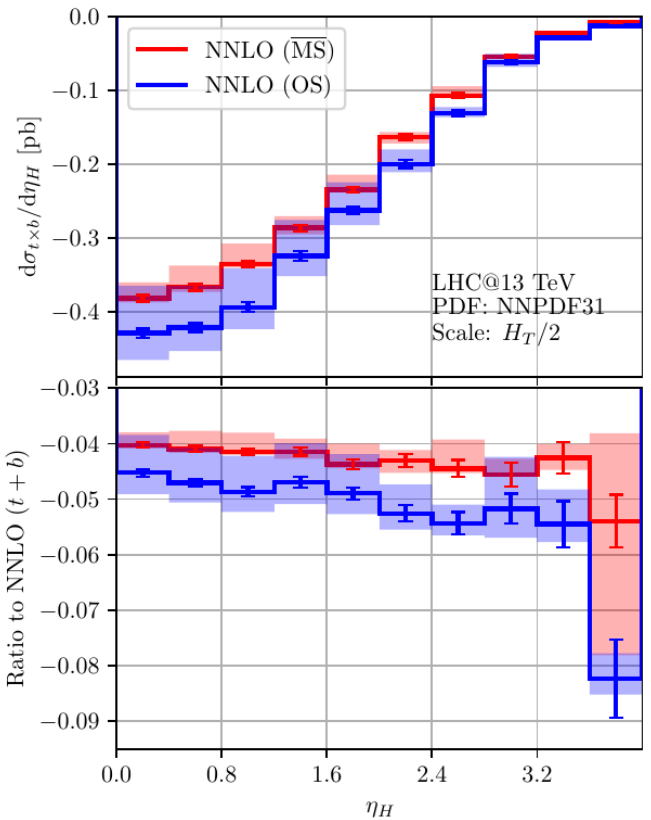

- p_T -distribution known (except for the zero-bin) and we find good agreement
  - Lindert et al., 2017
  - Caola et al., 2018
  - Bonciani et al., 2022
- Rapidity distributions constitute new results
- Mass-effects most notable at low p_T

Top-Bottom Interference Effects

$$H_T = \sqrt{m_H^2 + p_T^2} + \sum_i |p_{i,T}|$$

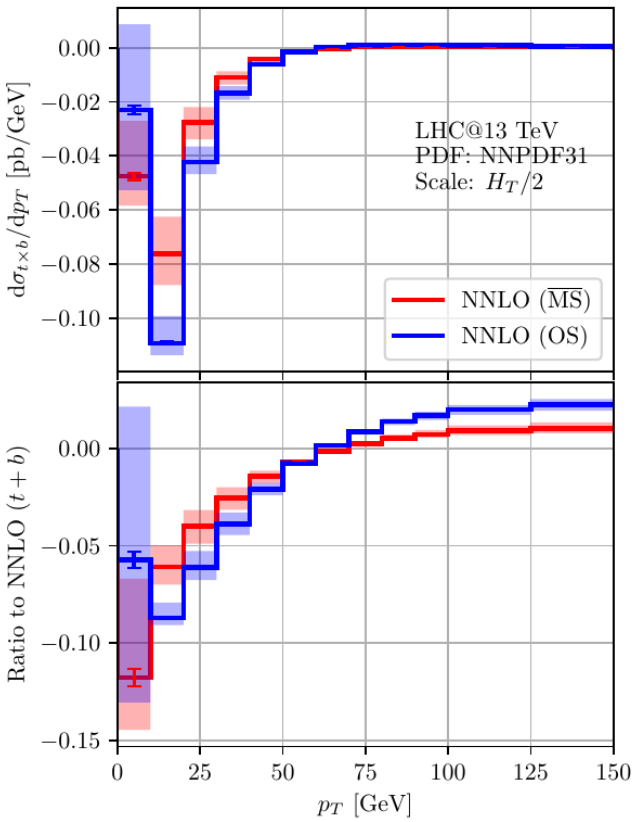

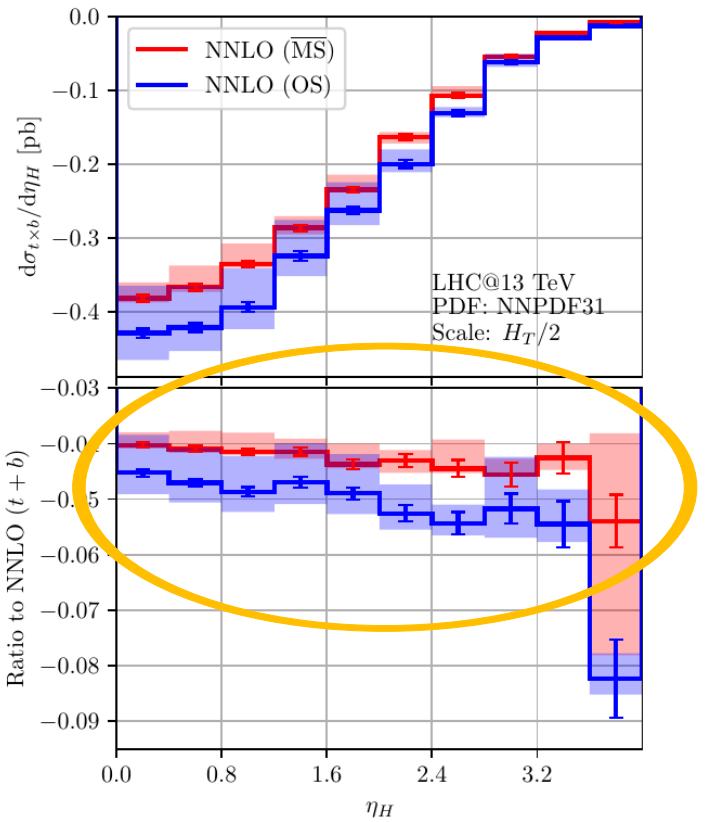

- p_T -distribution known (except for the zero-bin) and we find good agreement
  - Lindert et al., 2017
  - Caola et al., 2018
  - Bonciani et al., 2022
- Rapidity distributions constitute new results
- Mass-effects most notable at low p_T
- Mass-effects remain relatively constant in rapidity ($\sim$ -4% shift)

Distributions: HEFT vs. Full Theory

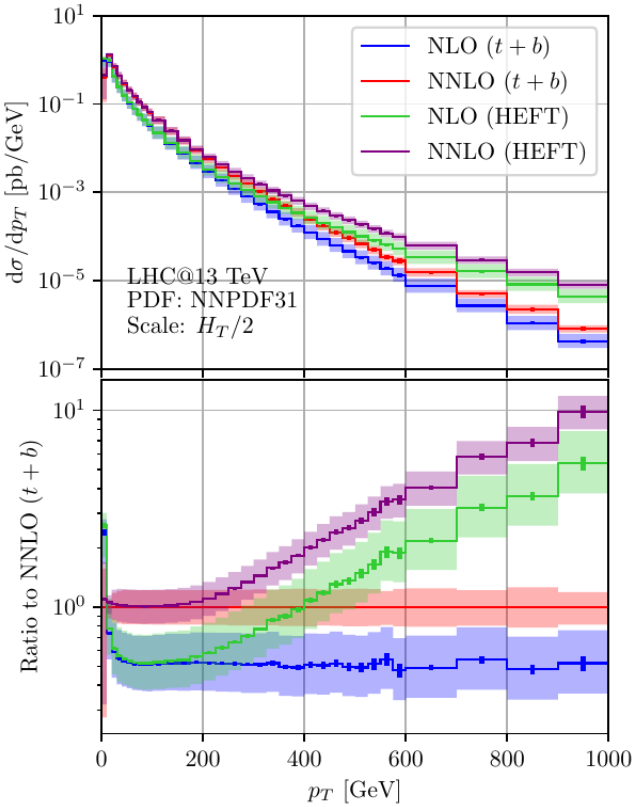

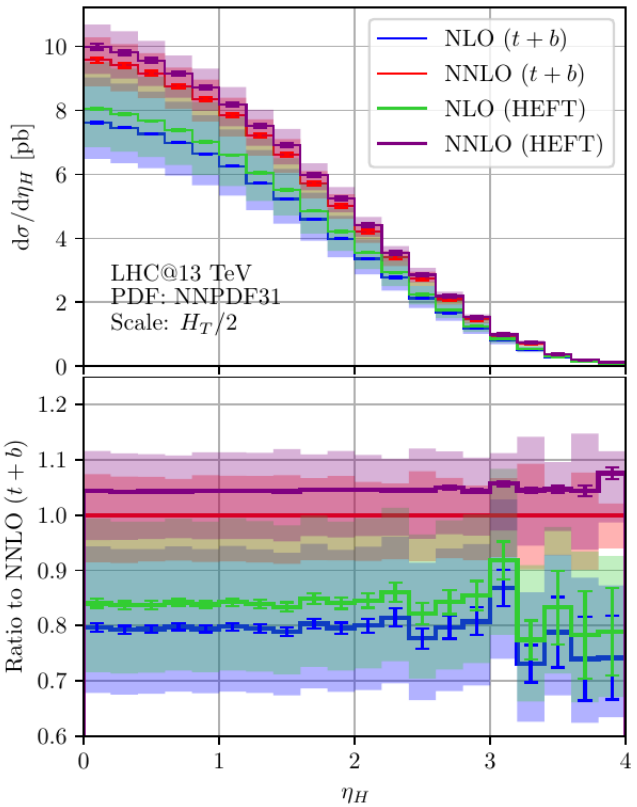

- Full theory: At very high p_T , p_T is the only relevant scale

$$d\sigma/dp_T^2 \sim 1/p_T^4$$

- Effective theory: dimensionful coupling

$$d\sigma/dp_T^2 \sim 1/(v^2 p_T^2)$$

Conclusions

- Complete analysis of top-bottom-interference effects on the Higgs production cross section at NNLO
- Addresses one of the leading theory uncertainties
- $\overline{\text{MS}}$ scheme shows better perturbative convergence and smalle scale uncertainties than OS scheme
- Good agreement between 4- and 5-flavor scheme
- Differential distributions, including novel rapidity spectra

$$\sigma_{ggH} = 48.81(1)^{+0.65}_{-2.02}(\text{N}^3\text{LO HEFT}) - 0.16^{+0.13}_{-0.03}(\text{NNLO } t) - 1.74(2)^{+0.13}_{-0.03}(\text{NNLO } t \times b) \text{ pb}.$$

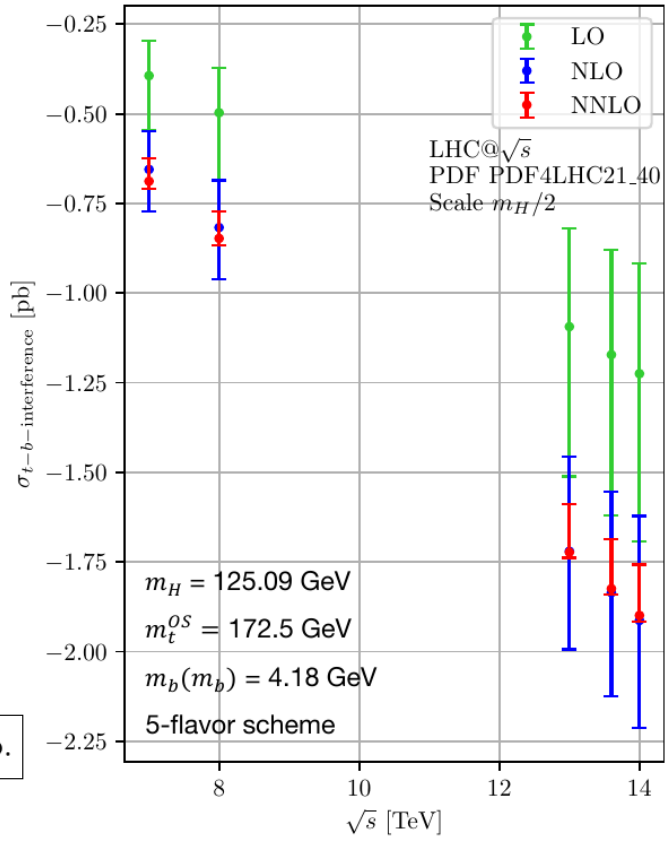

Conclusions

- Complete analysis of top-bottom-interference effects on the Higgs production cross section at NNLO
- Addresses one of the leading theory uncertainties
- $\overline{\text{MS}}$ scheme shows better perturbative convergence and smalle scale uncertainties than OS scheme
- Good agreement between 4- and 5-flavor scheme
- Differential distributions, including novel rapidity spectra

$$\sigma_{ggH} = 48.81(1)^{+0.65}_{-2.02}(\text{N}^3\text{LO HEFT}) - 0.16^{+0.13}_{-0.03}(\text{NNLO } t) - 1.74(2)^{+0.13}_{-0.03}(\text{NNLO } t \times b) \text{ pb}.$$

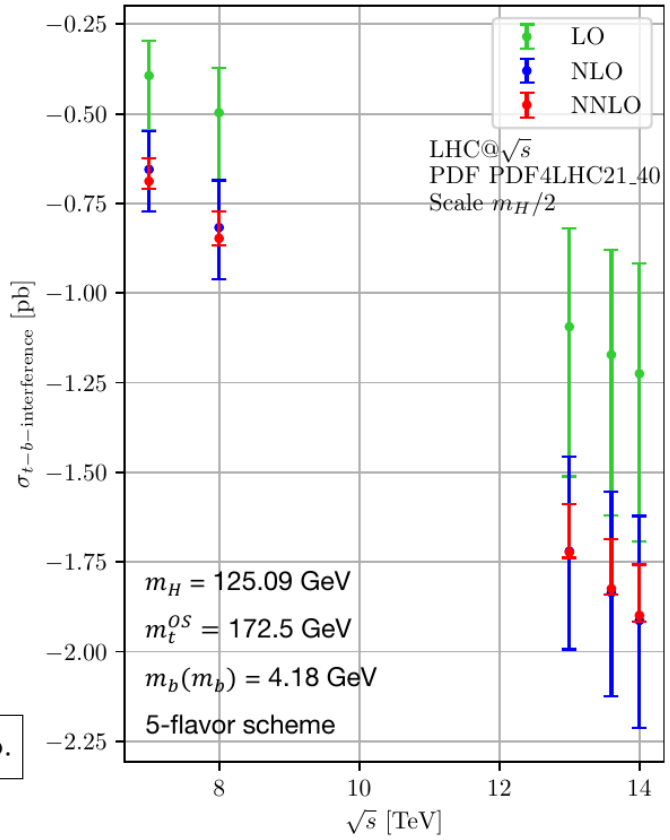

Thanks for your attention!

Backup

Top-Bottom Interference Contribution

Order	$\sigma_{t\times b}$ [pb]			
	$\sqrt{s} = 13$ TeV			
	5FS $m_t = 173.06$ GeV $\overline{m}_b(\overline{m}_b) = 4.18$ GeV	5FS $m_t = 173.06$ GeV $m_b = 4.78$ GeV	5FS $m_t(m_t) = 162.7$ GeV $\overline{m}_b(\overline{m}_b) = 4.18$ GeV	4FS $m_t = 173.06$ GeV $\overline{m}_b(\overline{m}_b) = 4.18$ GeV
$\mathcal{O}(\alpha_s^2)$	-1.11	-1.98	-1.12	-1.15
LO	$-1.11^{+0.28}_{-0.43}$	$-1.98^{+0.38}_{-0.53}$	$-1.12^{+0.28}_{-0.42}$	$-1.15^{+0.29}_{-0.45}$
$\mathcal{O}(\alpha_s^3)$	-0.65	-0.44	-0.64	-0.66
NLO	$-1.76^{+0.27}_{-0.28}$	$-2.42^{+0.19}_{-0.12}$	$-1.76^{+0.27}_{-0.28}$	$-1.81^{+0.28}_{-0.30}$
$\mathcal{O}(\alpha_s^4)$	$+0.02$	$+0.43$	-0.02	-0.02
NNLO	$-1.74(2)^{+0.13}_{-0.03}$	$-1.99(2)^{+0.29}_{-0.15}$	$-1.78(1)^{+0.15}_{-0.03}$	$-1.83(2)^{+0.14}_{-0.03}$

Finite Top-Quark Mass Effects

Order	$(\sigma_t - \sigma_{\text{HEFT}})$ [pb]	
	$\sqrt{s} = 13$ TeV	
	5FS $m_t = 173.06$ GeV	4FS $m_t = 173.06$ GeV $\overline{m}_b(\overline{m}_b) = 4.18$ GeV
LO	-	-
$\mathcal{O}(\alpha_s^3)$	-0.30	-0.27
NLO	$-0.30^{+0.10}_{-0.17}$	$-0.27^{+0.09}_{-0.16}$
$\mathcal{O}(\alpha_s^4)$	$+0.14$	$+0.12$
NNLO	$-0.16^{+0.13}_{-0.03}$	$-0.15^{+0.10}_{-0.02}$

Real-Virtual Corrections

- Variables: $\hat{s}, \hat{t}, \hat{u}, m_H^2, m_q^2$
- Introduce dimensionless variables and **fix ratio** m_q^2/m_H^2
  - z parametrizes soft limit
  - λ Parametrizes collinear limit

$$\hat{t}/\hat{s} = z\,\lambda \qquad \hat{u}/\hat{s} = z\,(1\text{-}\lambda)$$

$$z = 1\text{-}m_H^2/\hat{s} \qquad \lambda = \hat{t}/(\hat{t}+\hat{u})$$

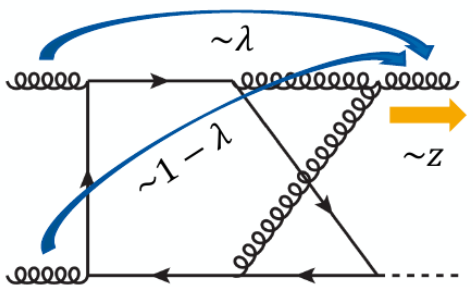

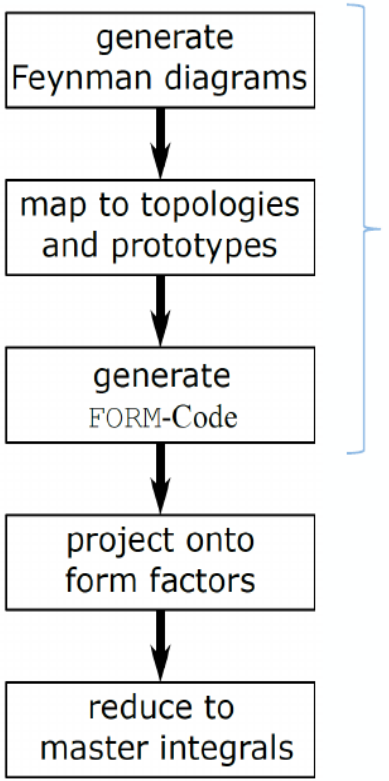

DiaGen
Czakon (private)

FORM
Vermaseren `00

Kira⊕FireFly
Klappert, Lange, et al. `20

- Solve master integrals with differential equation in m_q^2/m_H^2, z and λ
- Boundary condition $m_q^2/m_H^2 \to \infty$ with large mass expansion

Real-Virtual Corrections

- Create grid with numerical values of squared amplitude
- Subtract IR singularities:

$$\langle M^{(0)}_{gg\to Hg}|M^{(1)}_{gg\to Hg}\rangle\,|_{\text{regulated}} \equiv \langle M^{(0)}_{gg\to Hg}|M^{(1)}_{gg\to Hg}\rangle$$
$$- \left[r\,\langle M^{(0)}_{gg\to Hg,\text{HTL}}|M^{(1)}_{gg\to Hg,\text{HTL}}\rangle + \frac{8\pi\alpha_s}{\hat{t}}\langle P^{(0)}_{gg}\left(\frac{\hat{s}}{\hat{s}+\hat{u}}\right)\rangle\langle M^{(0)}_{gg\to H}|M^{(1)}_{gg\to H} - M^{(1)}_{gg\to H,\text{HTL}}\rangle\right]$$

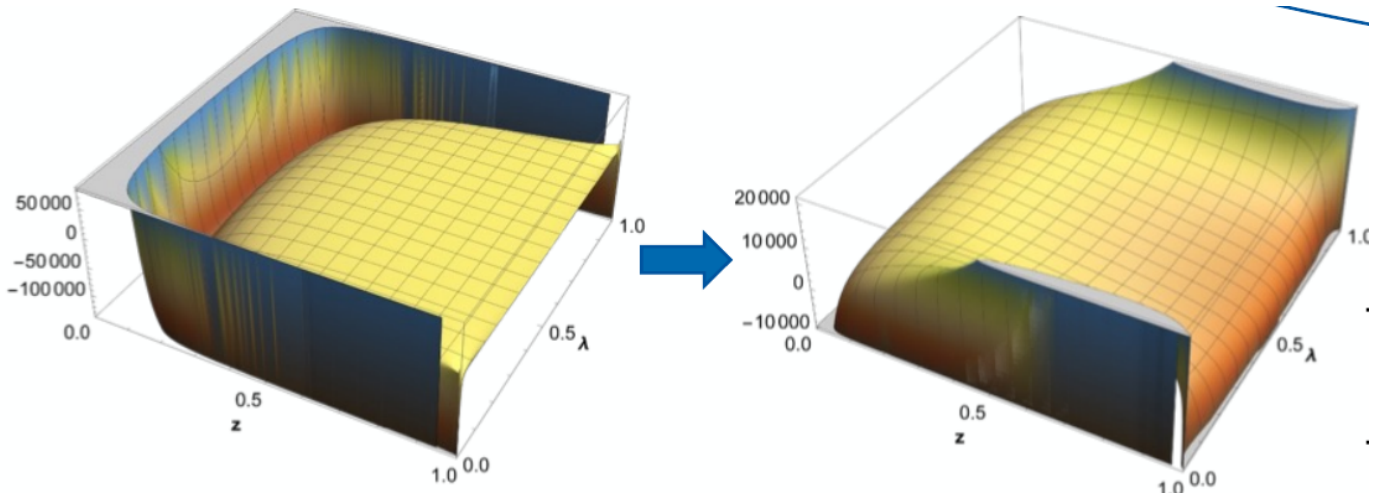

- Interpolate to any phace space point with cubic splines
- Add back subracted terms unsing analytical expressions

Evolution of differential equations

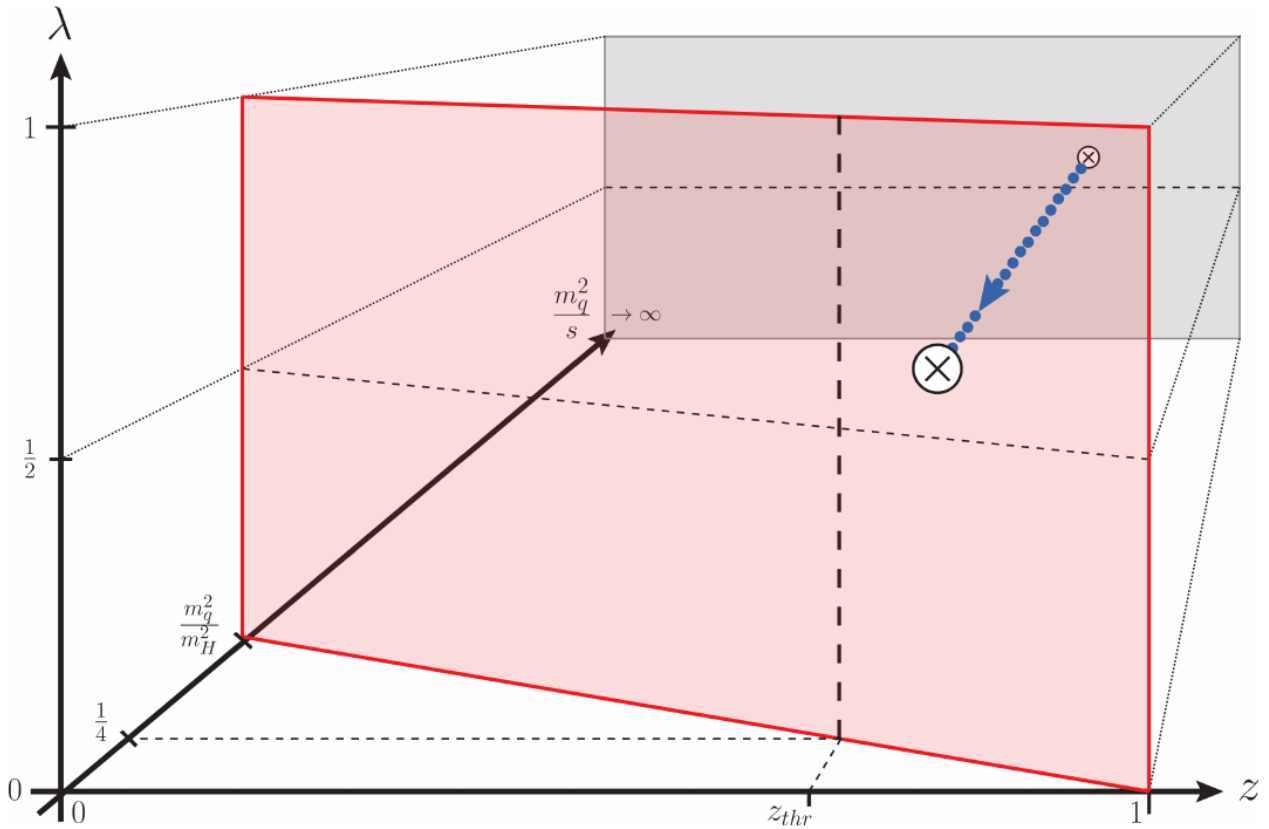

$z = 1\text{-}m_H^2/\hat{s}$

$\lambda = \hat{t}/(\hat{t}+\hat{u})$

$m_t^2/m_H^2 = 23/12$

Range of parameters:
- $\lambda \in (0,1)$
- $z \in (0,1)$

$z_{thr} = 1 - \frac{m_H^2}{4m_q^2}$

For $m_t^2/m_H^2 = 23/12$:
$z_{thr} = 20/23 \approx 0.87$

Evolution in the (z,λ)-plane

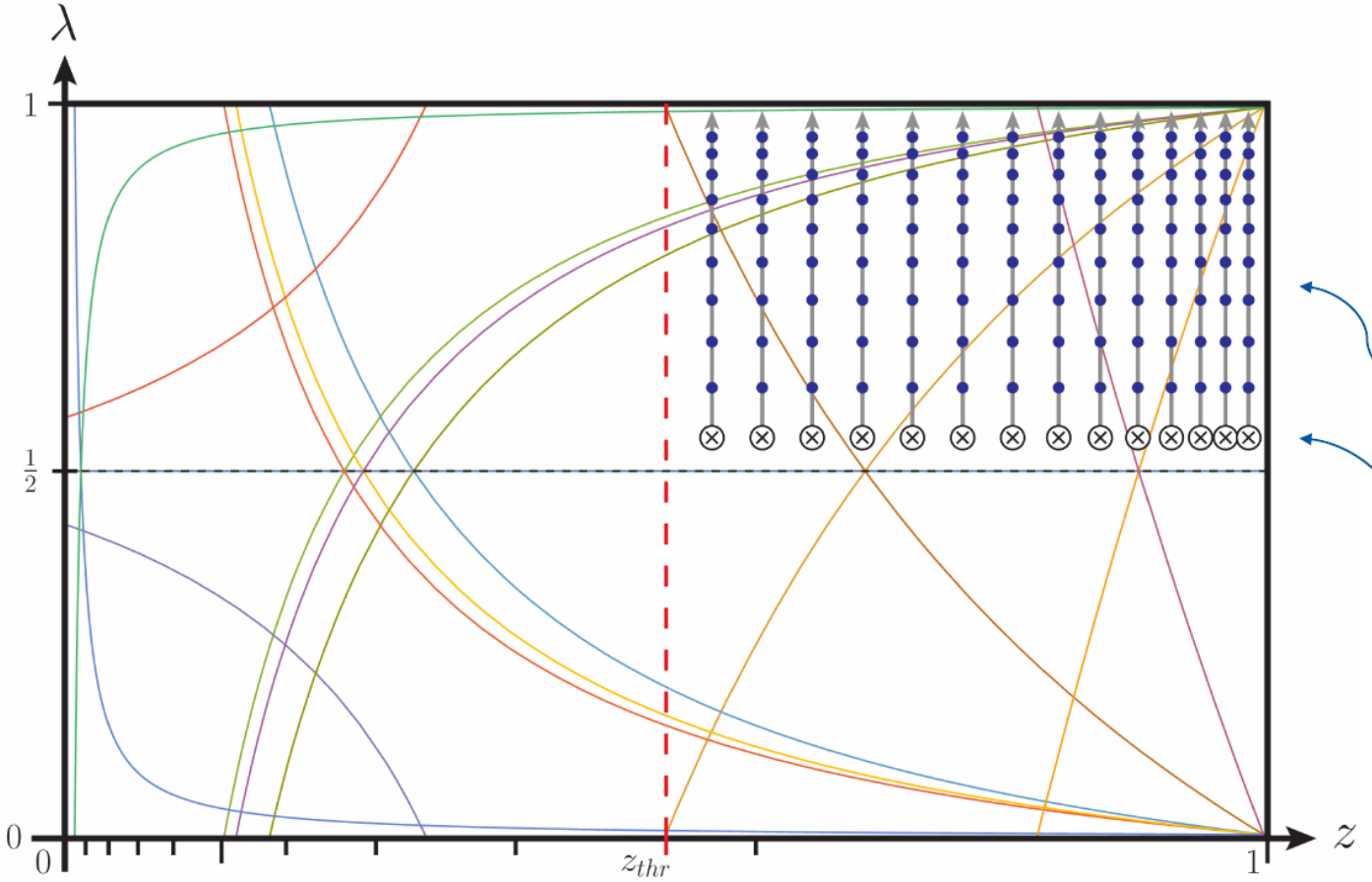

$z = 1\text{-}m_H^2/\hat{s}$

$\lambda = \hat{t}/(\hat{t}+\hat{u})$

$m_t^2/m_H^2 = 23/12$

Range of parameters:
- $\lambda \in (0,1)$
- $z \in (0,1)$

Collect numerical samples for MI along straight integration contours

Boundaries from numerical integration in the mass